Received: 21 October 2024 | Revised: 16 December 2024 | Accepted: 19 December 2024

DOI: 10.1111/andr.13837

ANDROLOGY

WILEY

ORIGINAL ARTICLE

A recurrent loss-of-function variant in *DRC1* causes non-syndromic severe asthenozoospermia with favorable intracytoplasmic sperm injection and pregnancy outcomes

Célia Tebbakh[1,2] | Anne-Laure Barbotin[3,4] | Guillaume Martinez[1,5] | Angèle Boursier[3,4] | Zeina Wehbe[1,5] | Asma Hammouda[1,2] | Nicolas Thierry-Mieg[6] | Christophe Arnoult[1] | Selima Fourati Ben Mustapha[7] | Raoudha Zouari[7] | Pierre F. Ray[1,2] | Zine-Eddine Kherraf[1,2]

[1]Institute for Advanced Biosciences, Team Genetics Epigenetics and Therapies of Infertility, University of Grenoble Alpes, Grenoble, France

[2]CHU Grenoble Alpes, UM GI-DPI, Grenoble, France

[3]CHU Lille, Laboratoire de Biologie de la Reproduction-Spermiologie-CECOS, Lille, France

[4]Development and Plasticity of the Neuroendocrine Brain, University of Lille, Lille, France

[5]CHU Grenoble Alpes, UM de Génétique Chromosomique, Grenoble, France

[6]CNRS, University of Grenoble Alpes, Grenoble, France

[7]Polyclinique les Jasmins, Centre d'Aide Médicale à la Procréation, Centre Urbain Nord, Tunis, Tunisia

Correspondence
Zine-Eddine Kherraf, Institute for Advanced Biosciences, Team Genetics Epigenetics and Therapies of Infertility, University of Grenoble Alpes, INSERM U1209, CNRS UMR 5309, Grenoble, France.
Email: ZEKherraf@chu-grenoble.fr

Funding information
University Grenoble Alpes; National Institute of Health and Medical Research; National Center of Scientific Research; Institute of Advanced Biosciences; French National Research Agency, Grant/Award Number: FLAGELOME ANR-19-CE17-0014

Abstract

Background: Asthenozoospermia, characterized by reduced sperm motility, is a common cause of male infertility. Multiple morphological abnormalities of the sperm flagella (MMAF) represent a severe and genetically heterogeneous form of asthenozoospermia. Over 50 genes have been associated, but approximately half of MMAF cases remain unexplained. DRC1, a gene involved in the nexin-dynein regulatory complex (N-DRC), has been linked to MMAF and primary ciliary dyskinesia (PCD), often with significant variability in clinical presentation.

Objectives: His study aimed to identify novel pathogenic *DRC1* variants in MMAF patients, assess their impact on sperm flagellar structure, and evaluate intracytoplasmic sperm injection (ICSI) and pregnancy outcomes.

Materials and methods: A cohort of 196 non-syndromic MMAF patients was analyzed using whole exome sequencing (WES). Functional validation of candidate variants included immunofluorescence to assess protein expression and transmission electron microscopy (TEM) to identify ultrastructural abnormalities. Assisted reproductive therapy outcomes were also evaluated.

Results: WES identified a recurrent homozygous frameshift variant in DRC1 NM_145038.5: c.109dup; p.(Gln37ProfsTer30) in four patients (2%), all of North African origin, none of whom suffer from PCD-related symptoms. The variant caused a complete absence of DRC1 protein in spermatozoa. TEM showed flagellar abnormalities, with 10% of axonemal sections revealing peripheral doublet dissociation, suggesting N-DRC instability. ICSI resulted in a 68.5% fertilization rate, with three out of four couples successfully delivering healthy children.

Discussion and conclusion: The identification of a novel and recurrent pathogenic DRC1 variant broadens the mutation spectrum associated with MMAF. The absence of systemic PCD symptoms suggests that DRC1 deficiency may primarily affect

spermatogenesis. Notably, the phenotypic spectrum might be influenced by the genetic background, varying across populations. Favorable ICSI outcomes, with a 68.5% fertilization rate and successful pregnancies in three out of four couples, highlight the effectiveness of assisted reproductive techniques for patients with this genetic defect.

KEYWORDS
asthenozoospermia, ccdc164, drc1, flagellum, male infertility, MMAF

1 | INTRODUCTION

Infertility affects an estimated 10%–20% of couples worldwide, with approximately 50 million of reproductive-aged couples, unable to conceive after 12 months or more of regular intercourse.[1] Male infertility contributes significantly to this issue, with a global prevalence ranging from 2% to 12%, and is implicated in 20%–70% of all infertility cases.[2] Given that up to 10% of the human coding sequences are dedicated to reproductive functions, it is unsurprising that genetic factors play a substantial role in male infertility, particularly when it comes to genes involved in sperm production and function.[3]

Sperm cells have specialized structures that are crucial for their role in fertilization. One of the most important is the flagellum, whose integrity is essential for sperm motility and fertilization.[4] The flagellum constitutes approximately 90% of the length of the sperm and contain a structure known as the 9 + 2 axoneme, which runs through its entire length, including the neck, middle, principal and end segments.[5] The axoneme consists of nine peripheral doublet microtubules (DMT) surrounding a central complex (CC) of two singlet microtubules. Each DMT is composed of multiple 96-nm units comprising identical sets of axonemal complexes like outer and inner dynein arms (ODAs and IDAs), radial spokes (RS) and the nexin-dynein regulatory complex (N-DRC). ODAs and IDAs are the molecular motors driving flagellar motility. ODAs generate high ciliary beat frequency, while IDAs control the bending shape of the flagella. The CC is connected to the nine DMTs through nine RS complexes that are believed to transmit a mechanochemical signal that locally controls dynein-driven microtubule sliding.[6]

Flagellum defects lead to reduced or absent sperm motility, a condition called asthenozoospermia, which is a common cause of male infertility. One of the most severe conditions of asthenozoospermia is multiple morphological abnormalities of the flagella (MMAF), a rare phenotype characterized by a mosaic of sperm morphological defects including absent, bent, short, irregular and coiled flagella.[4] MMAF is characterized by significant genetic diversity, with over 50 causative genes identified so far, yet approximately half of all cases remain unexplained.[7,8] This high rate of idiopathic cases highlights both the complexity of the molecular pathogeny underlying MMAF and the considerable potential for discovering additional genetic factors.

Herein, we investigated by whole exome sequencing (WES) a cohort of 196 infertile men displaying MMAF and identified a homozygous truncating variant in *DRC1*, a gene encoding a key component of the N-DRC. This variant (NM_145038.5: c.109dup) was found in four subjects (2%) of North African origin. Functional analysis using immunofluorescence (IF) showed a complete absence of DRC1 protein in sperm from patients carrying this variant, confirming its deleterious impact on protein expression and localization. Transmission electron microscopy (TEM) further demonstrated that while the primary assembly of the N-DRC is preserved, its stability is compromised, correlating with severe sperm morphological defects and motility impairments. These findings validate the pathogenicity of the identified variant and enhance our understanding of the genetic and structural bases of MMAF.

2 | MATERIAL AND METHODS

2.1 | Participant and ethical approval statement

This study respects all ethical guidelines (Declaration of Helsinki) and was approved by local ethics committees and the French Data Protection Authority (DR-2016-392) and samples collection (Fertithèque) was declared to the French Ministry of health (DC-2015-2580). An informed consent was obtained from all the subjects prior to their inclusion in the study.

2.2 Semen parameters and sperm morphology

Semen samples were obtained by masturbation after 2–7 days of sexual abstinence. Semen samples were incubated for 30 min at 37°C for liquefaction; ejaculate volume and pH, together with sperm concentration, vitality, morphology, and motility, were evaluated according to World Health Organization (WHO) guidelines.[9] Morphological abnormalities of the flagella as absent, bent, coiled, short, and irregular were recorded using an optical microscope observation.

2.2 | Transmission electron microscopy

To better characterize the impact of the reported candidate variant on sperm ultrastructure, sperm from a fertile control, and from patients P0705 and P0706 were subjected to TEM. Following fixation in 2.0% v/v glutaraldehyde in phosphate buffered saline (PBS, pH 7.4), the sperm pellet was washed for 15 min in fresh buffer containing 4% w/v sucrose, and embedded in 2% agar. Post-fixation was performed using

1% osmic acid in PBS. Samples embedded in agar were subsequently dehydrated in a graded series of ethanol. After dehydration, small pieces of agar containing spermatozoa were further embedded in Epon resin (Polysciences Inc., Warrington, PA, USA). Sections were cut on a Reichert OmU2 ultramicrotome (Reichert-Jung AG, Vienna, Austria) with a diamond knife. Ultrathin sections (70 nm) were collected on parlodion 0.8%/isoamyl acetate-coated 100 mesh Nickel grids (EMS, Fort Washington, PA, USA) and counterstained with 2% uranyl acetate and lead citrate before observation. Sections were examined with a Zeiss transmission electron microscope 902 (Leo, Rueil-Malmaison, France). Images were acquired using a Gatan Orius SC1000 CCD camera (Gatan France, Grandchamp, France).

2.3 | Whole exome sequencing and variant filtering

Sequencing of coding regions of all RefSeq isoforms and intron-exon junctions ± 5 bp with an Illumina NextSeq System after capture enrichment using Agilent SureSelect v7 Enrichment Reagents and KAPA HiFi HotStart ReadyMix kits. Raw data from the sequencer (bcl files) are converted to fastq format by the bcl2fastq v1.8.4 software (Illumina). The DNA sequences obtained are aligned to the GRCh38 reference genome by the BWAMEM software. Variations from the reference sequence are identified by the Strelka2 software. The detected variants are positioned, quantified, labeled, and ranked, then filtered according to their coverage rate, allelic frequency, transmission mode, impact on mRNA splicing and protein functional structure and according to the available bibliographic data. Variants are described according to the HGVS nomenclature (https://varnomen.hgvs.org) and classified, within the limits of current knowledge, as "pathogenic," "probably pathogenic," "benign," "probably benign," or "of uncertain significance" according to the recommendations of the American College of Medical Genetics and Genomics (ACMG) and the Association for Molecular Pathology (AMP).[10]

2.4 | Sanger verification

The candidate *DRC1* variant identified in subjects P0154, P0379, P0705, and P0706 was subjected to Sanger verification using an ABI 3500XL Genetic Analyzer (Thermo Fisher Scientific, Waltham, MA, USA). Analyses were performed using Sequence Scanner Software 2 (Applied Biosystems, Foster City, CA, USA). *DRC1* primer sequences (5′–3′), forward: GGGACTCCTGCCATGAATCC (T_m: 60.18°C) and, reverse: CCACCACGCCCGATTAATTG (T_m: 59.62°C).

2.5 | Immunofluorescence analysis of sperm cells

Immunostaining was carried out in triplicate on sperm cells from a fertile control subject and from individual P0706, displaying the MMAF phenotype and carrying the *DRC1* candidate variant. More than 100 cells were analyzed for each condition and marker. Sperm cells were fixed in PBS and 4% paraformaldehyde (PFA) for 7 min at room temperature. After washing in 1 mL PBS, the sperm suspension was spotted onto 0.1% poly L-lysine pre-coated slides (Thermo Fisher Scientific, Waltham, MA, USA). After attachment, sperm were permeabilized with 0.1% (v/v) Triton X-100-DPBS (Triton X-100; Sigma-Aldrich Co., Ltd., Irvine, UK) for 5 min at RT. Slides were then blocked in 5% normal serum–DPBS (normal goat or donkey serum; GIBCO, Thermo Fisher Scientific) and incubated overnight at 4°C with the primary antibodies: rabbit polyclonal anti-DRC1 (BS-15149R, ThermoFisher Scienfitic, 1:100), anti DRC2 (24376-1-AP, Proteintech, 1:100), anti DRC4 (HPA041311, Human Protein Atlas, 1:100) and guinea-pig anti-acetylated-α-tubulin (AA345-GP, Geneva Antibody Facility, 1:400). Washes were performed with 0.1% (v/v) Triton X-100-DPBS, followed by 1 h incubation at room temperature with secondary antibodies. Highly cross-adsorbed goat secondary antibodies (Alexa Fluor 568 nm anti-rabbit IgG, IgG (A11036, 1:800) and Alexa Fluor 488 nm anti-guinea-pig IgG (A11073, 1:800)) were purchased from ThermoFischer Scientific. Appropriate controls were performed, omitting the primary antibodies. Samples were counterstained with 5 mg/mL Hoechst 33342 (Sigma–Aldrich) and mounted with DAKO mounting medium (Thermo Fisher Scientific). Fluorescence images were captured with a confocal microscope (Zeiss LSM 710).

2.6 | Intracytoplasmic sperm injection procedure

Each woman's partner were submitted to controlled ovarian hyperstimulation (COH) as previously described.[11] Several ovarian protocol were used depending on the age of women, the ovarian reserve, and previous response to COH. Oocyte retrieval was performed 36 h after ovulation triggering. Following oocyte recovery, a decoronization by both chemical (80 IU/mL hyaluronidase in Flushing, FertiPro) and mechanical methods (successive aspirations and expulsions of oocytes with a micropipette) was performed. On the day of the intracytoplasmic sperm injection (ICSI), a semen sample was obtained and carrying-out using a density gradient technique.[12] ICSI was performed by preferentially selecting progressive motile or non-progressive motile spermatozoa as alternative. The ICSI procedure was performed using an inverted microscope (Leica DMI8, Leica Microsystems, Germany) and Narishige micromanipulators. Fertilization was assessed 16–18 h after injection. Fertilized oocytes were cultured in culture medium (CSCM-C, Fujifilm IrvineSicentific, Santa Ana, CA, USA) at 37°C under the following gas conditions 5% CO_2, 5% O_2, and 90% N_2. Until the time of transfer (Day 2, 3, or 5 depending of the center). Embryo or blastocyst quality was checked prior to transfer, which was done under ultrasound supervision. Viable blastocyst obtained at day 5 were cryopreserved

2.7 | Outcomes measures

The fertilization rate was calculated as the ratio of oocytes exhibiting two pronuclei divided by the number of injected mature oocytes.

The blastocyst development rate was defined by the number of blastocysts on day 5 divided by the number of normally fertilized oocytes for further culture (ESHRE Special Interest Group of Embryology and Alpha Scientists in Reproductive Medicine, 2017) Clinical pregnancy was defined as the presence of a gestational sac on ultrasonography at 6 weeks of gestation. All pregnancies were followed up until delivery.

3 | RESULTS

3.1 | Whole exome sequencing identified a recurrent homozygous truncating variant in DRC1

In a cohort of 196 individuals with MMAF analyzed using WES, we identified a recurrent homozygous frameshift variant, c.109dup, in the *DRC1* gene (NM_145038.5) in four subjects (P0154, P0379, P0705, and P0706) (Figure 1A). All four patients present with isolated infertility, with no associated symptoms suggestive of primary ciliary dyskinesia (PCD). Their medical history and clinical evaluations do not reveal any respiratory issues, recurrent infections, or other common manifestations typically associated with PCD. Their condition appears to be limited to reproductive challenges without evidence of the systemic symptoms often seen in PCD cases. All of these individuals were of North African descent, indicating the likelihood of a shared common ancestor. This variant is rare in the general population with minor allele frequency (MAF) $< 0.1\%$ (3.15×10^{-5}) in gnomAD v4 with no homozygous detected among the 806,247 sequenced subjects. The higher MAF value was observed in the Middle Eastern population (4.94×10^{-4}), which highly shares ancestory with the North African population.

This variant is located in the downstream sequence of exon 1 of the gene, 49 bp from the donor splice site. Both SpliceAI and SPiP (score 0.044) predicted no effect on splicing. The predicted impact of this variant is to introduce a frameshift resulting in a premature termination codon in exon 2/17, thus leading either to the degradation of the abnormal mRNA by the nonsense-mediated decay (NMD) mechanism or the production of a truncated and non-functional protein (p.(Gln37ProfsTer30)) displaying only 5% of the wild-type sequence size (Figure 1B). Loss-of-function variants in *DRC1* have been described as pathogenic, being implicated in PCD and asthenozoospermia.[13,14] While this specific variant has been documented in the ClinVar germline database as pathogenic or likely pathogenic (Variation ID: 663966, Accession: VCV000663966.9), it has not yet been reported in the literature in individuals with PCD/MMAF-related conditions.

Overall, we identified here by WES a novel and rare homozygous frameshift variant in the upstream coding region of the *DRC1* gene, which has been previously associated with asthenozoospermia. This variant likely explains the infertility observed in our patients. Further, we present functional evidence supporting the pathogenicity of this variant, enabling its classification as pathogenic (Class V) according to ACMG criteria.

3.2 | Immunofluorescence experiments evidenced loss of DRC1 expression in sperm from patients carrying the candidate variant

To confirm the deleterious impact of the candidate *DRC1* variant at the protein level, we conducted IF experiments in triplicate ($n = 3$) using an antibody raised against DRC1. For these experiments, we used available sperm samples from patient P0706, who has a homozygous *DRC1* mutation, as well as from fertile control subjects (> 100 sperm cells were observed for each condition). In the control sperm, we observed a strong DRC1 IF signal along the full length of the flagellum, indicating its proper expression and localization (Figure 2). In contrast, sperm from patient P0706 showed no detectable DRC1 signal in the flagellum. This absence confirms that the mutation severely disrupts the normal expression and localization of DRC1 in the sperm flagellum. These results clearly demonstrate that the *DRC1* variant prevents the normal expression and localization of the encoded protein, highlighting the mutation's significant impact on the structure and function of the sperm flagellum and its involvement in MMAF and male infertility.

3.3 | DRC1 deficiency results in multiple morphological abnormalities of the sperm flagella due to N-DRC instability and MTD dissociation

Sperm from patients carrying the *DRC1* mutation were first assessed using optical microscopy, before and after fixation and staining. This analysis revealed several disrupted parameters, including severe motility impairments and significant morphological abnormalities. Morphologically normal spermatozoa were almost completely absent, with only about 0.5% (± 1) displaying a typical structure, underscoring the presence of severe teratozoospermia. Specifically, 51% (± 29.7) showed flagellar abnormalities such as absent (18% ± 3.5), short (32.2% ± 16.5), coiled (23.7% ± 7.0), and irregular caliber (37.2% ± 26.7) (Table 1). These observations strongly indicate asthenozoospermia caused by MMAF (Figure 3A).

To gain deeper insights into the ultrastructural defects contributing to the abnormal sperm morphology observed in this patient, TEM analysis was performed. The study focused on sperm samples from subjects P0705 and P0706, carrying the homozygous candidate *DRC1* variant, as well as from control fertile subjects for comparison. Compared to controls, sperm from P0705 and P0706 showed abnormalities in several structural components (Figure 3B). Nuclear vacuoles were present in approximately 10% of the heads. The midpieces displayed an organized and well-arranged mitochondrial sheath, but many exhibited a reduced helix structure. Approximately, 30% of the midpieces contained hypertrophic residual bodies with a reduced number of hypertrophic mitochondria, and occasionally, supernumerary nuclear membranes. Flagella showed elongation defects in about 20%–30% of the longitudinal sections examined. Regarding axonemal structures, 90% of the observed cross-sections revealed a normally formed axoneme with a typical 9+2 arrangement, including both external and

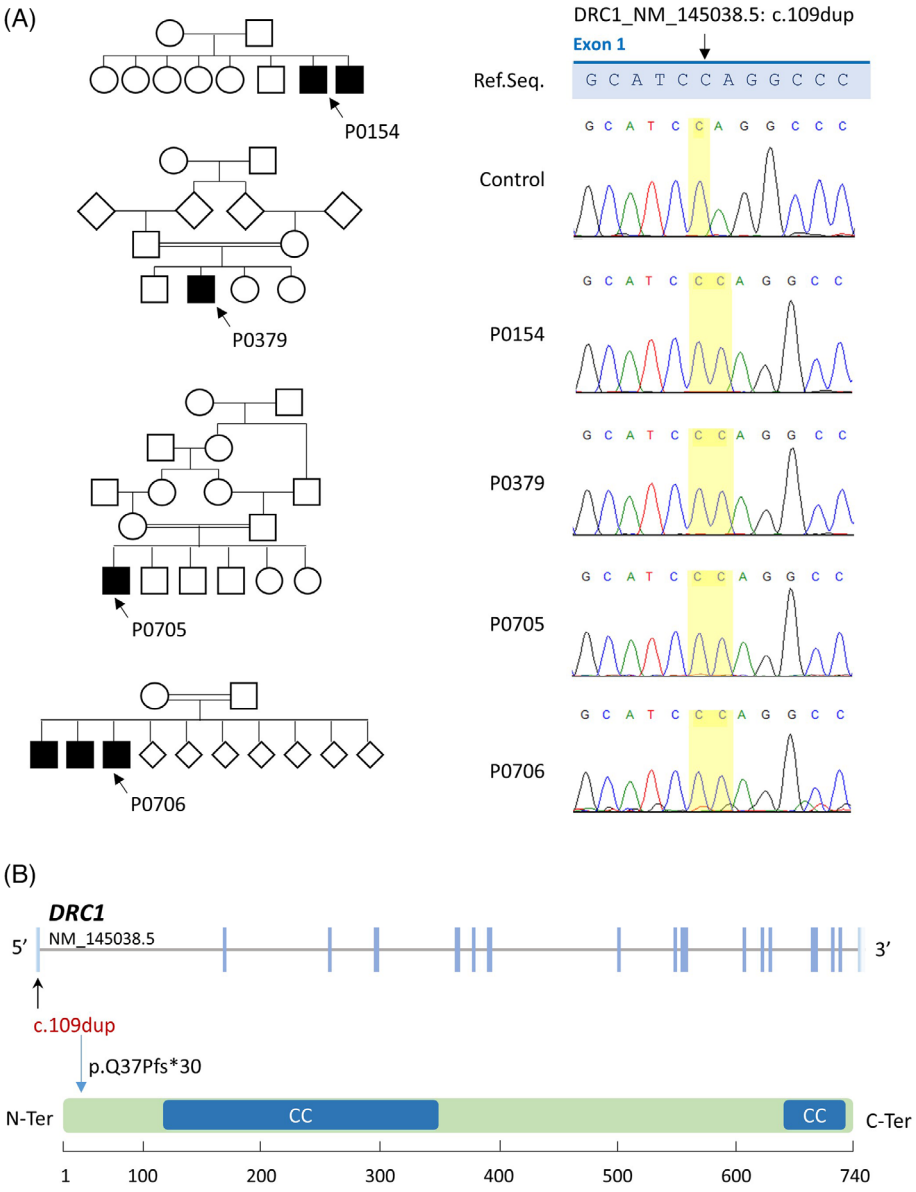

FIGURE 1 Identification of a Homozygous DRC1 Variant in four patients of the MMAF cohort (2%). (A) Pedigree charts and Sanger sequencing electropherograms related to four MMAF patients carrying the candidate variant. Each panel corresponds to one of the patients, demonstrating the variant's presence in both alleles. (B) Schematic representation of the DRC1 gene with the position of the homozygous variant (c.109dup) indicated. This frameshift mutation is located in exon 1 and introduces a premature termination codon, resulting in a truncated protein lacking its main structural and functional domains. CC, Coiled coil. DRC, Dynein regulatory complex; MMAF, multiple morphological abnormalities of the sperm flagella.

internal dynein arms. However, in 10% of the sections, an incomplete axoneme was observed, characterized by the dissociation of the peripheral doublets suggesting the absence of one or more N-DRC. Peri-axonemal structures showed that the dense fibers were well-arranged, with the fibrous sheath appearing of normal thickness to moderately thickened and irregular in about one-third of the sections. The longitudinal columns were normally visible.

In conclusion, sperm from patients carrying the *DRC1* mutation exhibit a significant proportion of abnormalities consistent with defects in the N-DRC, aligning with the genetic diagnosis. These structural abnormalities are closely associated with impaired sperm function, particularly affecting motility, as evidenced by the observed asthenozoospermia.

3.4 | DRC1 plays a crucial role in maintaining the stability and function of the N-DRC but is dispensable for its primary assembly

To elucidate the role of DRC1 in the assembly and stability of N-DRC, we conducted IF experiments in triplicate ($n = 3$) using antibodies targeting two key components of the N-DRC: DRC2 and DRC4, implicated

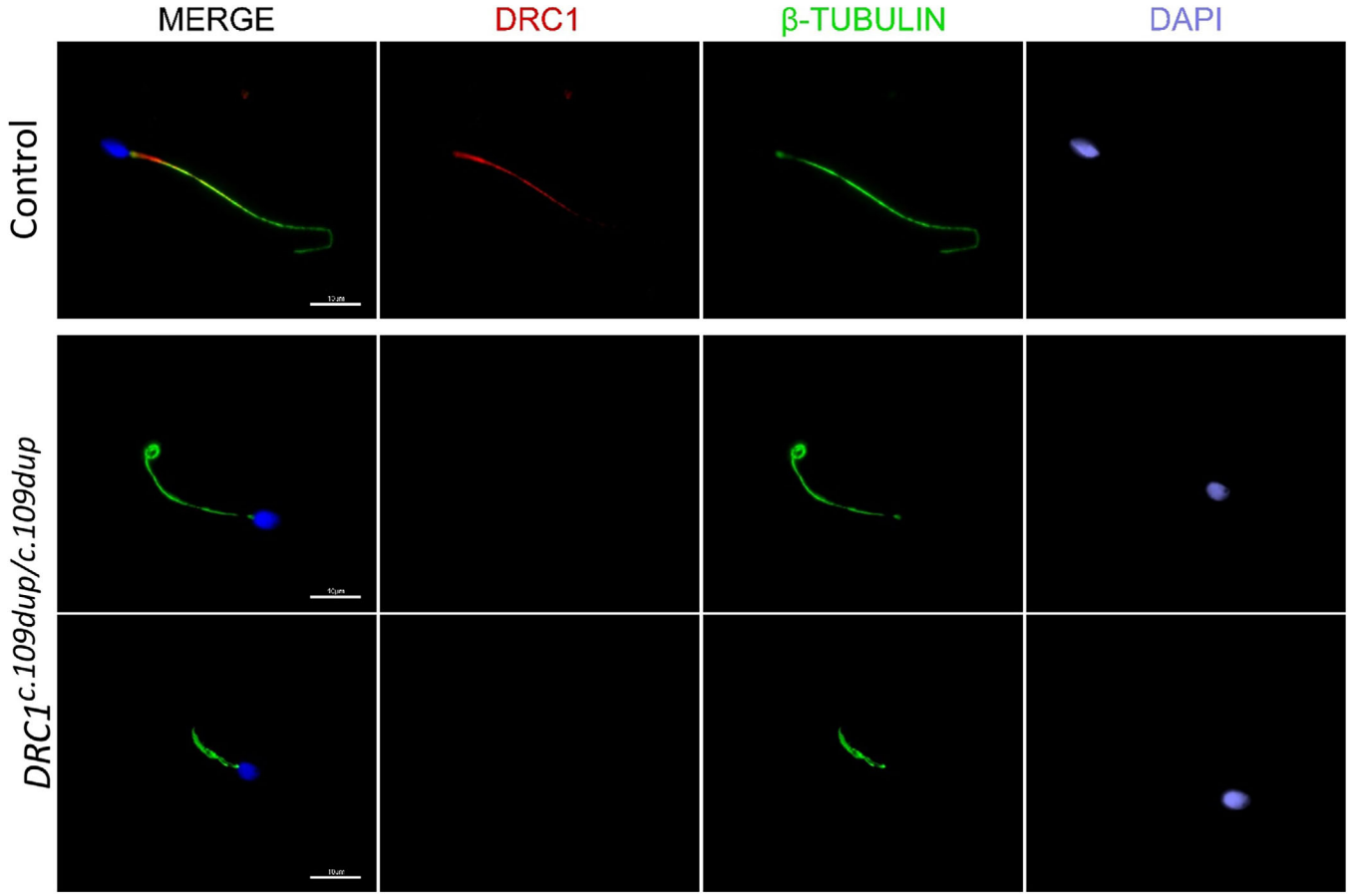

FIGURE 2 Immunofluorescence analysis of DRC1 expression in spermatozoa DRC1 immunofluorescence staining demonstrates the absence of DRC1 protein in spermatozoa from the patient carrying the homozygous DRC1 mutation compared to a fertile control. Spermatozoa were labeled with polyclonal anti-DRC1 antibody (red) to visualize DRC1 localization. Anti-acetylated α-tubulin antibody (green) was used to highlight the axonemal microtubules, and DNA was counterstained with 4′,6-diamidino-2-phenylindole, DAPI (blue) for nuclear visualization. The figure contrasts the strong DRC1 signal in the fertile control with the complete lack of DRC1 signal in the patient's sperm. This analysis was performed in triplicate ($n = 3$), with over 100 sperm cells analyzed for each condition. DRC, Dynein regulatory complex.

TABLE 1 Semen parameters of the four patients carrying the *DRC1* variant.

Semen parameters	Reference range*	P0154	P0379	P0705	P0706	Average
Age (years)		42	36	22	33	33.3 (± 8.4)
Sperm volume (mL)	≥1.4	2	3.4	4.33	4.61	3.6 (± 1.2)
Sperm concentration (10^6/mL)	≥16	12	38.5	10	6.85	16.8 (± 14.6)
Total motility (%)	≥42	10	2	12	15	9.7 (± 5.6)
Progressive motility (%)	≥30	5	0	2	5	3.0 (± 2.4)
Vitality (%)	≥54	60	65	27	52	51.0 (± 16.9)
Normal spermatozoa (%)	>4	0	0	0	2	0.5 (± 1.0)
Flagella abnormalities (%)**	NA	100	100	72	30	75.5 (± 33.1)
Absent	≤5	20	20	14	0	18.0 (± 3.5)
Short	≤1	36	54	19	20	32.2 (± 16.5)
Coiled	≤17	16	24	33	22	23.7 (± 7.0)
Irregular caliber	≤2	64	56	19	10	37.2 (± 26.7)
Multiple	≤1	0	2	0	0	0.7 (± 1.1)

Note: *Semen parameter reference values were obtained from the WHO 2021 guidelines. **Reference limits for sperm flagella abnormalities were based on the distribution range of morphologically normal spermatozoa observed in 926 fertile men.[15] The average is presented as the mean of the values ± the standard deviation.

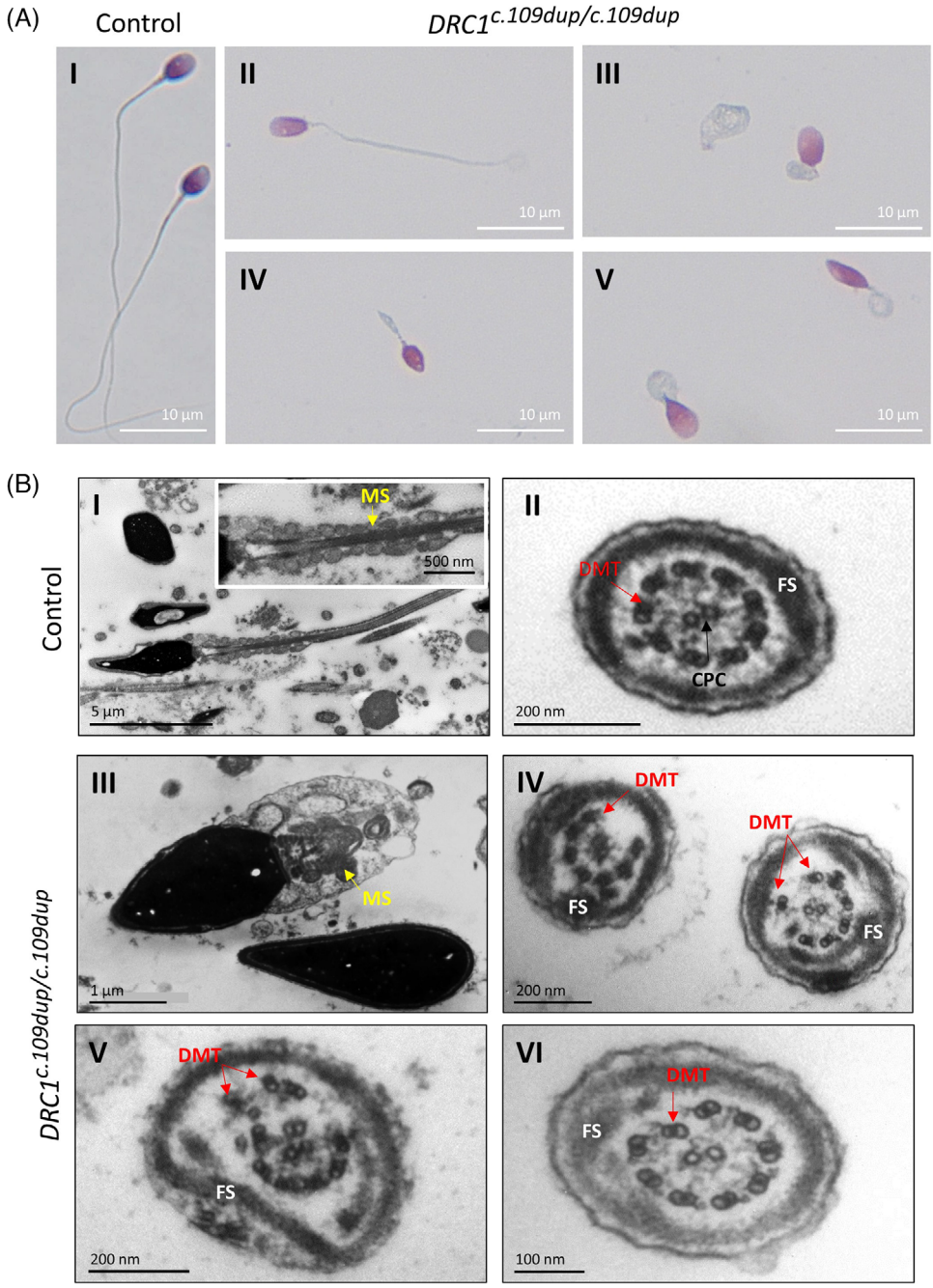

FIGURE 3 Transmission electron microscopy (TEM) of spermatozoa from DRC1 Variant Carriers. (A) Shorr staining of sperm from control and patients carrying the DRC homozygous c.109dup variant. (B) Representative TEM sections of spermatozoa from control and patients with the homozygous c.109dup DRC1 variant. Notable differences in the axonemal structure are highlighted, including disorganized mitochondrial sheaths and the presence of abnormal or incomplete axonemes. MS, Mitochondrial sheath; FS, fibrous sheath; CPC, central pair complex; DMT, doublet microtubules; DRC, nexin-dynein regulatory complex.

with DRC1 in the formation of the N-DRC core structure.[16] These experiments were performed on available sperm samples from patient P0706, who carries a homozygous DRC1 variant, and compared with fertile control sperm (> 100 sperm cells were observed for each condition and marker). In the sperm samples from patient P0706, like in controls, IF signals for DRC2 and DRC4 were clearly present and uniformly distributed along the length of the axoneme (Figure 4). This indicates that the primary assembly of the N-DRC, remains intact in the absence of DRC1. However, the presence of DRC1 is crucial for maintaining the stability and proper function of the N-DRC.

3.5 | Intracytoplasmic sperm injection outcomes

The outcomes of ICSI procedures for the four patients with the DRC1 homozygous variant are summarized in Table 2. None of the cycles

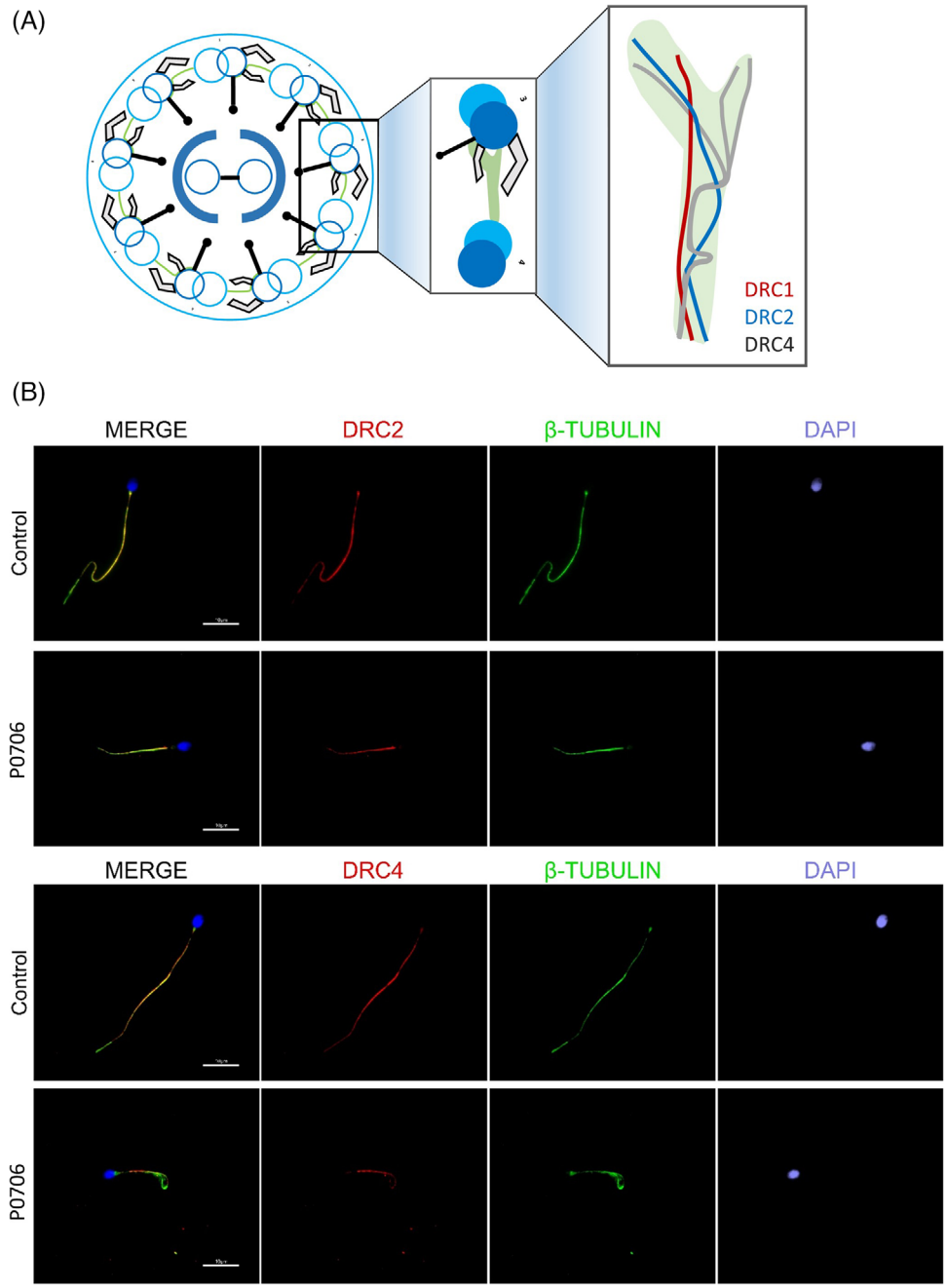

FIGURE 4 Conservation of N-DRC Components in the absence of DRC1. (A) Diagram depicting the N-DRC complex and its subunit interactions, illustrating the position and role of DRC1 within the complex. The schematic highlights the interactions between DRC1, DRC2, and DRC4 as part of the regulatory scaffold essential for axonemal function. (B) Immunofluorescence staining of spermatozoa from a patient with the DRC1 mutation, showing the localization of DRC2 and DRC4. Spermatozoa were stained with polyclonal anti-DRC2 and anti-DRC4 antibodies (red) and anti-acetylated α-tubulin (green) to visualize the axoneme. DNA was counterstained with DAPI (blue). This analysis was performed in triplicate ($n = 3$), with over 100 sperm cells analyzed for each condition and marker (DRC2 and DRC4). N-DRC, Nexin-dynein regulatory complex.

required the use of an HOS test for oocyte injection. The overall fertilization rate was satisfactory at 68.5 ± 14.8, closely aligning with the benchmark threshold (ESHRE Special Interest Group of Embryology and Alpha Scientists in Reproductive Medicine, 2017). All ICSI attempts produced embryos suitable for transfer, and three out of the four couples achieved clinical pregnancies.

At the first clinic, patients P0154 and P0379 each underwent two ICSI cycles. For P0154, two embryos (D2-3) were transferred in the first cycle, but no clinical pregnancy resulted. In the second cycle, two fresh blastocysts were transferred, leading to a clinical pregnancy and the birth of one child. Additionally, transferring two frozen embryos resulted in another clinical pregnancy and the birth of another child.

TABLE 2 ICSI outcomes in patients carrying the homozygous *DRC1* (c.109Dup) variant.

Clinical Characteristics	P0154		P0379		P0705	P0706	Average all cycles
ICSI cycles	ICSI 1	ICSI 2	ICSI 1	ICSI 2	ICSI 1	ICSI 1	
Male age (years)	38	43	36	37	22	34	35.0 ± 7.0
Female age (years)	24	29	33	34	21	34	29.2 ± 5.6
No. of oocytes retrieved	8	23	11	8	24	14	14.7 ± 7.2
No. of oocytes injected	6	17	6	5	22	12	11.3 ± 7.0
No of injected oocytes	6	17	6	5	22	12	11.3 ± 7.0
No. of zygotes	4	16	3	3	16	8	8.3 ± 6.2
Fertilization rate (%)	66.7	94	50	60	73	67	68.5 ± 14.8
Total no. of D2–D3 embryos	4	16	3	3	16	8	8.3 ± 6.2
Early development rate (%)	100	100	100	100	100	100	100.0 ± 0.0
Total no. of blastocysts	NA	9	NA	NA	9	4	7.3 ± 2.9
Blastoformation rate (%)	NA	56	NA	NA	56.2	50	54.1 ± 3.5
Number of frozen blastocyst	NA	3	NA	NA	9	4	5.3 ± 3.2
No. of D2 or D3 embryo transferred	2	NA	2	2	NA	NA	2.0 ± 0.0
No. of blastocyst transferred	NA	2 + 2*	NA	NA	1*	1*	1.5 ± 0.6
Clinical pregnancy	0	1+1	0	0	1	1	0.6 ± 0.5
Live birth	NA	1+1	NA	NA	1	1	1.0 ± 0.0

Notes: The average is presented as the mean of the values ± the standard deviation.
*Frozen embryo transfer.

For P0379, both ICSI cycles involved transferring two embryos (D2-3) each time, but neither cycle resulted in a clinical pregnancy.

At the second clinic, patients P705 and P706 experienced ovarian hyperstimulation syndrome (OHSS), which prevented fresh embryo transfers on day 5. Consequently, all viable blastocysts were frozen for later transfer. Each couple underwent a single frozen embryo transfer, and both resulted in pregnancies and live births on the first attempt.

4 | DISCUSSION

Herein, investigation by WES of a cohort of 196 patients led to the identification of a recurrent homozygous frameshift variant (c.109dup) in *DRC1*, a gene encoding for a critical component of the N-DRC and previously linked to asthenozoospermia and male infertility in human and mouse.[13,14,17] The variant identified in this study was found in four individuals of North African descent, suggesting a shared genetic background and possible common ancestry. The rarity of this variant in the general population, with an MAF < 0.1%, and its higher frequency in the Middle Eastern population, which shares genetic similarities with North Africans, supports the notion of a founder effect. The variant is located in exon 1 and introduces a frameshift leading to a premature termination codon in exon 2. This alteration likely results in the degradation of the mRNA through NMD. Previous studies have established that loss-of-function mutations in *DRC1* are pathogenic and associated with PCD and asthenozoospermia. While this specific variant has been classified as probably pathogenic in the ClinVar database, its role in *DRC1*-related conditions had not been documented in the literature prior to this study. IF analysis was used to evaluate the impact of the *DRC1* variant at the protein level. In control sperm samples, DRC1 exhibited a strong and uniform signal along the entire length of the flagellum, indicating proper expression and localization. In stark contrast, sperm from patient P0706, who carries the homozygous *DRC1* mutation, showed no detectable DRC1 signal. This absence confirms that the variant severely disrupts the expression and localization of DRC1, thereby impairing its function in the sperm flagellum. These results align with the observed clinical phenotype, highlighting the mutation's substantial impact on sperm structure and function. Finally, in line with ACMG criteria, functional evidence from this study supports the classification of this variant as pathogenic (class V).

To investigate the structural defects in DRC1-deficient sperm, we examined the axonemal structures using TEM and IF microscopy. TEM provided detailed insights into the structural abnormalities, revealing the extent of the defects at a subcellular level. Although the majority of sperm heads and midpieces exhibited normal chromatin and mitochondrial arrangements, significant abnormalities were still observed in other regions. These included reduced mitochondrial helix structure, hypertrophic residual bodies, and elongation defects in the flagella. Although 90% of axonemal cross-sections revealed a typical 9+2 arrangement, 10% exhibited incomplete axonemes with missing or dissociated N-DRC units. The peri-axonemal structures were mostly normal, though some sections showed irregularities. These observations confirm that the identified *DRC1* mutation leads to instability and functional disruption of the N-DRC, contributing to the observed flagellar defects and asthenozoospermia.

IF experiments targeting other key-N-DRC components, DRC2 and DRC4, were conducted to further investigate the role of DRC1. The analysis revealed that DRC2 and DRC4 signals were present and uniformly distributed in sperm from both patient P0706 and control subjects. This suggests that DRC1 is not essential for the primary assembly of the N-DRC but is crucial for maintaining its stability and function. These results are consistent with our TEM findings, which showed that while N-DRC assembly was present, its integrity was compromised in the patients' samples. These findings are also consistent with those of Zhang et al.,[14] who identified bi-allelic loss-of-function variants in the *DRC1* gene in two unrelated individuals from China with non-syndromic infertility associated to MMAF.[14] Sperm from these patients showed disordered microtubule arrangements, underscoring the critical role of DRC1 in maintaining the integrity of the axonemal structure. Further, Zhang et al. used the CRISPR/Cas9 technology to generate two knock-in mouse lines reproducing the *DRC1* mutations identified in their patients. Analysis of flagellum formation dynamics during spermiogenesis revealed that while axoneme assembly occurred normally in early-stage spermatids, the microtubules within these cells became increasingly disorganized as spermatids differentiated. In the mutated animals, this disorganization progressed to the point where a normal axonemal structure was no longer present, highlighting the essential role of DRC1 in regulating the structural stability of sperm flagellar axonemes.

In contrast to the findings of Zhang et al., who reported a complete absence of DRC2 and DRC4 in Drc1-mutant mouse sperm based on IF experiments, our study demonstrated normal expression and localization of these N-DRC subunits in human mutant sperm. This discrepancy likely reflects species-specific differences in DRC1 function and its contextual roles. Zhang et al. also highlighted distinct morphological and substructural defects between sperm flagella and cilia in mice, as well as phenotypic variability depending on the mouse strain, ranging from asthneozoospermia and male infertility to hydrocephaly and even prepubertal death. These phenotypic differences highlight the limitations of mouse models in fully recapitulating human pathophysiology. Compared to these models, our findings emphasize the specific role of DRC1 in the assembly and stabilization of the human sperm flagellum. In addition, while Zhang et al. reported ICSI outcomes for one patient and a single ICSI cycle, limiting conclusions about the clinical management, our study provides a more comprehensive analysis. We recorded ICSI outcomes for all four couples in our study, including data from two cycles and two embryo transfer when applicable. Notably, we documented live births, providing practical and clinically relevant information about the impact of DRC1 variants on fertility treatment outcomes.

Due to the conserved axonemal structure between motile cilia and sperm flagella, asthenozoospermia may be part of PCD (#MIM 244400), a genetic multisystemic disorder characterized by impaired ciliary function, leading to chronic sinopulmonary disease that could be associated in 50% of cases with a situs inversus totalis which is referred to as the Kartagener syndrome.[18] However, many infertile men carrying pathogenic variants in ciliopathy-related genes displayed mild PCD-symptoms or isolated asthenozoospermia, highlighting their wide phenotypic expression variability. A recent study carried-out by Yiallouros et al. performed a fine description of the genotype–phenotype correlation in a series of PCD-patients carrying mutations in *RSPH9*, a well-established causative gene in PCD.[19] They showed that RSPH9 mutations were associated with a wide phenotypic variability even in patients bearing the same variant. Another study conducted by Zhang et al. revealed that genetic background is a key determinant of PCD pathogenesis.[14] In their study, they generated several *Drc1* mutant mouse strains and observed that the phenotypic manifestations were dependent to the strain. Overall, these data underscore the fact that differences in genetic background may influence the penetrance of different PCD-related mutations. Moreover, previous studies in humans have reported inconsistent correlations between DRC1 deficiency and the severity of PCD when analyzing genotype–phenotype correlations. For instance, deletions in exons 1–4 of the *DRC1* gene were found to be common in East Asian populations, especially among Japanese and Korean PCD patients.[20–22] The Japanese patients tended to have milder symptoms with subtle ciliary alterations than the Korean patients who often experienced severe and rapid decline in lung function.[23] In our study, all four patients presented displayed an isolated MMAF phenotype without other PCD manifestations, such as chronic respiratory issues or sinus infections. This absence emphasizes the specific effect of the genetic variant on spermatogenesis and male fertility without broader systemic involvement.

One of the key limitations of our study is the lack of complementary pulmonary investigations, such as nasal nitric oxide (NO) measurements or ciliary beat frequency analysis using High-Speed Video Analysis (HSVA). Although no respiratory symptoms were reported by the patients upon extensive questioning,[24] these additional assessments could have provided deeper insights into the potential involvement of ciliary dysfunction. However, these tests were not performed as the patients declined further exploration. It is worth noting that while DRC1 mutations have been associated with respiratory symptoms, the extent and severity of these symptoms can vary significantly across different populations. Previous studies, such as Raidt et al.,[25] have demonstrated that DRC1 mutations can result in a normal ciliary beat frequency, with overlapping values observed in control subjects. Nevertheless, the same study also identified subtle abnormalities in the ciliary beat pattern, such as a stiffer beat characterized by reduced ciliary beat amplitude. This mild phenotype could easily be overlooked or misinterpreted as normal. Despite these limitations, our findings contribute to the understanding of the phenotypic variability associated with DRC1 mutations and highlight the need for further studies incorporating comprehensive pulmonary assessments to better characterize the spectrum of associated clinical manifestations.

In conclusion, our study identifies a novel homozygous *DRC1* variant that contributes to MMAF through its impact on sperm morphology and function. The absence of DRC1 protein in patient sperm and the resultant structural abnormalities highlight the critical role of DRC1 in maintaining the stability and function of the N-DRC. While DRC1 is not essential for the initial assembly of the N-DRC, it is indispensable for the complex's stability and proper functioning. This comprehensive analysis underscores the significant impact of the *DRC1* mutation

on male fertility and provides important insights into the molecular mechanisms underlying asthenozoospermia. Furthermore, identifying PCD-related genotypes in the context of male infertility can aid in managing patients and preventing disease progression. Additionally, through appropriate genetic counseling, it is possible to identify at-risk family members, even during asymptomatic periods or early disease stage. This can potentially prevent the development of PCD, while also facilitating the early diagnosis and management of infertility in male relatives.

AUTHOR CONTRIBUTIONS

Célia Tebbakh, Pierre F. Ray, and Zine-Eddine Kherraf analyzed the data and wrote the manuscript. Anne-Laure Barbotin, Selima Fourati Ben Mustapha, and Raoudha Zouari provided clinical samples. Célia Tebbakh, Asma Hammouda, Christophe Arnoult, Nicolas Thierry-Mieg, Pierre F Ray, and Zine-Eddine Kherraf performed and analyzed the genetic data. Anne-Laure Barbotin and Angèle Boursier performed TEM analysis and analyzed the ultrastructural data. Guillaume Martinez, Zeina Wehbe, and Célia Tebbakh performed immunofluorescence experiments and analyzed their data. Pierre F. Ray and Zine-Eddine Kherraf designed the study, supervised all molecular laboratory work, had full access to all data in the study, and took responsibility for the integrity of the data and its accuracy. All authors have read and agreed to the published version of the manuscript

ACKNOWLEDGMENTS

We thank all the individuals for their cooperation, as well as all the referring physicians. This work was supported by the University Grenoble Alpes (UGA), the National Institute of Health and Medical Research (INSERM), the National Center of Scientific Research (CNRS), the Institute of Advanced Biosciences (IAB), and the French National Research Agency (grant FLAGELOME ANR-19-CE17-0014).

CONFLICT OF INTEREST STATEMENT

The authors declare no conflicts of interest.

DATA AVAILABILITY STATEMENT

Data sharing not applicable to this paper as no datasets were generated or analyzed during this study.

ORCID

Guillaume Martinez https://orcid.org/0000-0002-7572-9096
Pierre F. Ray https://orcid.org/0000-0003-1544-7449
Zine-Eddine Kherraf https://orcid.org/0000-0003-0351-6689

REFERENCES

1. Vander Borght M, Wyns C. Fertility and infertility: definition and epidemiology. *Clin Biochem*. 2018;62:2-10.
2. Eisenberg ML, Esteves SC, Lamb DJ, et al. Male infertility. *Nat Rev Dis Primer*. 2023;9:1-22.
3. Murat F, Mbengue N, Winge SB, et al. The molecular evolution of spermatogenesis across mammals. *Nature*. 2023;613:308-316.
4. Mortimer D. The functional anatomy of the human spermatozoon: relating ultrastructure and function. *Mol Hum Reprod*. 2018;24:567-592.
5. Lindemann CB, Lesich KA. Functional anatomy of the mammalian sperm flagellum. *Cytoskelet Hoboken NJ*. 2016;73:652-669.
6. Smith EF, Yang P. The radial spokes and central apparatus: mechano-chemical transducers that regulate flagellar motility. *Cell Motil Cytoskeleton*. 2004;57:8-17.
7. Stallmeyer B, Dicke A-K, Tüttelmann F. How exome sequencing improves the diagnostics and management of men with non-syndromic infertility. *Andrology*. 2024; 1-14. doi:10.1111/andr.13728
8. Touré A, Martinez G, Kherraf Z-E, et al. The genetic architecture of morphological abnormalities of the sperm tail. *Hum Genet*. 2021;140:21-42.
9. World Health Organization. *WHO Laboratory Manual for the Examination and Processing of Human Semen*. 6th ed. WHO Press; Switzerland. 2021;Available from: https://www.who.int/publications/i/item/9789240030787
10. Richards S, Aziz N, Bale S, et al. Standards and guidelines for the interpretation of sequence variants: a joint consensus recommendation of the American College of Medical Genetics and Genomics and the Association for Molecular Pathology. *Genet Med*. 2015;17:405-424.
11. Barbotin A-L, Boursier A, Jourdain A-S, et al. Identification of a novel CFAP61 homozygous splicing variant associated with multiple morphological abnormalities of the flagella. *J Assist Reprod Genet*. 2024;41:1499-1505.
12. Boursier A, Boudry A, Mitchell V, et al. Results and perinatal outcomes from 189 ICSI cycles of couples with asthenozoospermic men and flagellar defects assessed by transmission electron microscopy. *Reprod Biomed Online*. 2023;47:103328.
13. Wirschell M, Olbrich H, Werner C, et al. The nexin-dynein regulatory complex subunit DRC 1 is essential for motile cilia function in algae and humans. *Nat Genet*. 2013;45:262-268. doi:10.1038/ng.2533
14. Zhang J, He X, Wu H, et al. Loss of DRC1 function leads to multiple morphological abnormalities of the sperm flagella and male infertility in human and mouse. *Hum Mol Genet*. 2021;30:1996-2011.
15. Auger J, Jouannet P, Eustache F. Another look at human sperm morphology. *Hum Reprod*. 2016;31:10-23.
16. Gui L, Song K, Tritschler D, et al. Scaffold subunits support associated subunit assembly in the Chlamydomonas ciliary nexin-dynein regulatory complex. *Proc Natl Acad Sci U S A*. 2019;116:23152-23162.
17. Oud MS, Houston BJ, Volozonoka L, et al. Exome sequencing reveals variants in known and novel candidate genes for severe sperm motility disorders. *Hum Reprod Oxf Engl*. 2021;36:2597-2611.
18. Wei S, Xie H, Cheng Y. Progress in diagnosis of primary ciliary dyskinesia. *J Paediatr Child Health*. 2022;58:1736-1740.
19. Yiallouros PK, Kouis P, Pirpa P, et al. Wide phenotypic variability in RSPH9-associated primary ciliary dyskinesia: review of a case-series from Cyprus. *J Thorac Dis*. 2019;11:2067-2075.
20. Keicho N, Hijikata M, Morimoto K, et al. Primary ciliary dyskinesia caused by a large homozygous deletion including exons 1–4 of DRC1 in Japanese patients with recurrent sinopulmonary infection. *Mol Genet Genomic Med*. 2020;8:e1033.
21. Morimoto K, Hijikata M, Zariwala MA, et al. Recurring large deletion in DRC1 (CCDC164) identified as causing primary ciliary dyskinesia in two Asian patients. *Mol Genet Genomic Med*. 2019;7:e838.
22. Takeuchi K, Xu Y, Kitano M, et al. Copy number variation in DRC1 is the major cause of primary ciliary dyskinesia in the Japanese population. *Mol Genet Genomic Med*. 2020;8:e1137.
23. Oh J, Lee J-S, Park MS, et al. Diagnosis of primary ciliary dyskinesia via whole exome sequencing and histologic findings. *Yonsei Med J*. 2024;65:48-54.
24. Behan L, Dunn Galvin A, Rubbo B, et al. Diagnosing primary ciliary dyskinesia: an international patient perspective. *Eur Respir J*. 2016;48:1096-1107.
25. Raidt J, Wallmeier J, Hjeij R, et al. Ciliary beat pattern and frequency in genetic variants of primary ciliary dyskinesia. *Eur Respir J*. 2014;44:1579-1588.

26. Ben Khelifa M, Coutton C, Zouari R, et al. Mutations in DNAH1, which encodes an inner arm heavy chain dynein, lead to male infertility from multiple morphological abnormalities of the sperm flagella. *Am J Hum Genet*. 2014;94:95-104.
27. ESHRE Special Interest Group of Embryology and Alpha Scientists in Reproductive Medicine. The Vienna consensus: report of an expert meeting on the development of ART laboratory performance indicators. *Reprod Biomed Online*. 2017;35:494-510.

How to cite this article: Tebbakh C, Barbotin A-L, Martinez G, et al. A recurrent loss-of-function variant in *DRC1* causes non-syndromic severe asthenozoospermia with favorable intracytoplasmic sperm injection and pregnancy outcomes. *Andrology*. 2025;13:2110–2121.
https://doi.org/10.1111/andr.13837